

Parabolic Approximation Line Search: An efficient and effective line search approach for DNNs

Maximus Mutschler and Andreas Zell
University of Tübingen
Sand 1, D-72076 Tübingen, Germany

{maximus.mutschler, andreas.zell}@uni-tuebingen.de

Abstract

This work shows that line searches performed only over the loss function defined by the current batch can successfully compete with common optimization methods on state-of-the-art architectures in wall clock time. In other words, our approach is performing competitively, despite for the most part ignoring the noise originating from batch sampling of the loss function. Furthermore, we empirically show that local minima on lines in direction of the negative gradient can be estimated almost perfectly by a parabolic approximation. This suggests that the loss function is at least locally convex, which mitigates the common perception of a highly non convex loss landscape. Our approach combines well-known methods such as parabolic approximation, line search and conjugate gradient, to perform an efficient line search. To evaluate general performance as well as the hyper parameter sensitivity of our optimizer, we performed multiple comprehensive hyperparameter grid searches on several datasets and architectures. In addition, we provide a convergence prove on a simplified scenario. PyTorch and Tensorflow implementations are provided at <https://github.com/cogsys-tuebingen/PAL>.

1. Introduction

Mahsereci and Hennig [22] as well as Kafka and Wilke [17] introduced line search approaches for DNNs which are directly applied on discontinuous stochastic loss functions: $L(\mathbf{x} : \theta)$ where \mathbf{x} is a batch sampled from the distribution defined by a dataset. The realization of line searches in a discontinuous scenario is hard since multiple losses on a line have to be measured to approximate the expected loss on this line. Despite multiple losses are measured at different positions of a line, these approaches are competitive to basic SGD without momentum [26] [22][17]. In contrast to these line searches, our approach applies the line search not on the noisy loss function, but directly on the continuous loss function defined by one batch. In other words, we ignore the noise completely and assume successfully that the location of a minimum on a line in negative gradient direction of one batch is a well enough estimator for the minimum of the stochastic loss function to perform a successful optimization process.

To get an intuition of how the loss function of one batch on a line in negative gradient direction is shaped, we used Goodfellow’s et al.’s linear interpolation method to analyze and plot loss values on a line [11]. Surprisingly, we found that these lines behave locally almost like parabolas, as is exemplified in Figure 1. Elaborating this property we can perform an almost optimal line search by approximation

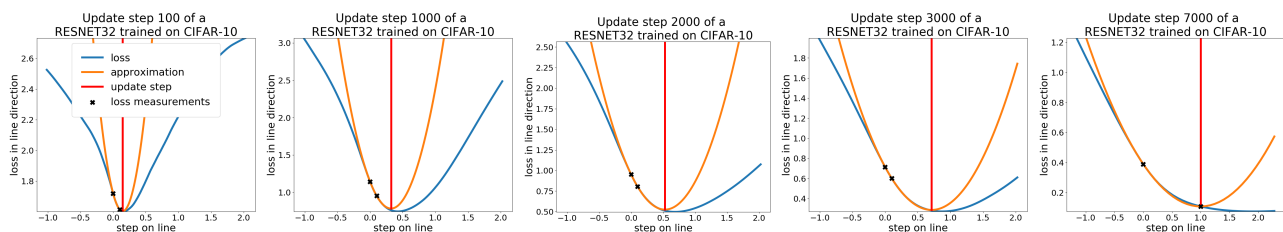


Figure 1: Loss function on lines in negative gradient direction (blue) combined with our parabolic approximation (orange) and the location of the minimum (red). The unit of the horizontal axis is $\|g\|$. Further line plots are provided in Appendix D.

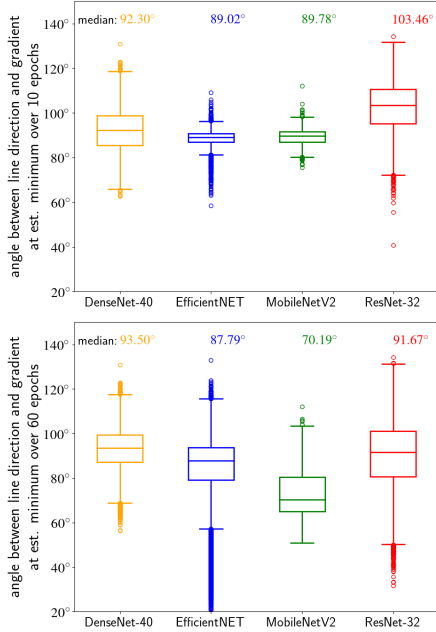


Figure 2: Angles between the line direction and the gradient at the estimated minimum measured on the same batch. If the angle is 90° , the estimated minimum is a real local minimum. We know from additional line plots that the found extrema or saddle points are minima. Top: measurement over the first 10 epochs. Bottom: Measurement over the first 60 epochs. The update step adaptation described in Section 2.3 is applied.

the loss function in negative gradient direction by a one-dimensional parabolic function ($f(x) = ax^2 + bx + c$) and then performing an update step to the minimum of this approximation. To do this, we only need to measure one additional point on the same batch.

To evaluate the validity of this property, we measure the gradient at the location of the estimated minimum during the training process with our line search. A position is a local extremum or saddle point of the line if and only if the angle between the line direction and the gradient at the position is 90° , if measured on the same batch. This holds because if the directional derivative of the measured gradient in direction of the line is 0, the current position is an extremum or saddle point of the line and the angle is 90° . If the position is not an extremum or saddle point, the directional derivative is not 0. As shown in Figure 2 (top) this property holds very well for the first 10 epochs when training several architectures on CIFAR10. Figure 2 (bottom) shows that the property gets slightly less accurate when we continue training for additional 50 epochs. The reason is, that the local shapes of the lines tend to have flatter regions around the minimum, as can be seen in the last line plot of Figure 1. We can ensure that the found extrema are minima,

as we also plotted the loss line for each update step. The utilization of the described empirical results, in addition to some further features leads to our proposed optimization method **Parabolic Approximation Line Search (PAL)**. A description of our line search approach, including its update rule as well as additional features, is given in section 2. Section 3 theoretically analyses convergence under the assumption that each intersection of a loss function is a parabolic function. In Section 4 we provide an extensive overview over related work. Section 5 empirically shows that *PAL* can compete with other optimization methods on several state-of-the-art network architectures and datasets. Section 6 and 7 provide a comprehensive discussion and outlook.

2. The line search algorithm

2.1. Parameter update rule

An intuitive explanation of *PAL*'s parameter update rule, based on a parabolic approximation, is given in Figure 3. Let the loss function be $L(x_t; \theta_t)$ where x_t is the input vector and θ_t are the parameters to be optimized at optimization step t . $L(x_t; \theta_t)$ may include random components, but, to ensure continuity during one line search, the same random numbers have to be used for each value determination of L . The gradient g_t is defined by $\nabla_{\theta_t} L(x_t; \theta_t)$. The loss $l(s)$ on a line in the direction of the negative normalized gradient is

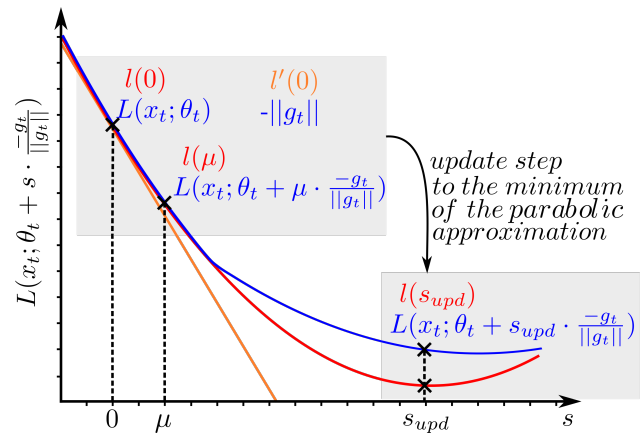


Figure 3: Basic idea of *PAL*'s parameter update rule. The blue curve is the loss function on a line in direction of the negative gradient at $L(x_t; \theta_t)$. It is defined by $l(s) = L(x_t; \theta_t + s \cdot \frac{-g_t}{\|g_t\|})$ where g_t is $\nabla_{\theta_t} L(x_t; \theta_t)$. The red curve is its parabolic approximation. With $l(0)$, $l(\mu)$ and g_t (orange), we have the three parameters needed to determine the update step s_{upd} to the minimum of the parabolic approximation.

therefore given by:

$$l(s) = L(x_t; \theta_t + s \cdot \frac{-g_t}{\|g_t\|}) \quad (1)$$

Since $l(s)$ is assumed to be a parabolic function it has the form $l(s) : \mathbb{R} \rightarrow \mathbb{R}, l(s) = as^2 + bs + c$ with $a \neq 0$. We need three points to define a, b and c . Those are given by the current loss $l(0)$, the derivative in gradient direction $l'(0) = -\|g_t\|$ and an additional loss $l(\mu)$ with measuring distance μ . We get $a = \frac{l(\mu) - l(0) - l'(0)\mu}{\mu^2}$, $b = l'(0)$, and $c = l(0)$. The update step s_{upd} to the minimum of the parabolic approximation is thus given by:

$$s_{upd} = -\frac{l'(0)}{l''(0)} = -\frac{b}{2a} = -\frac{l'(0)}{2\frac{l(\mu) - l(0) - l'(0)\mu}{\mu^2}} \quad (2)$$

Note that $l''(0)$ is the second derivative of the approximated parabola and is only identical to the exact directional derivative $\frac{-g_t}{\|g_t\|} H(L(x_t; \theta_t)) \frac{-g_t^T}{\|g_t\|}$ if the parabolic approximation

Algorithm 1 *PAL*, our proposed line search algorithm for deep neural networks. See Section 2 for details.

Input: Hyperparameters: μ : measuring step size,
 α : update step adaptation, β : conjugate gradient factor
 s_{max} : maximum step size.

Input: $L(x; \theta)$: loss function

Input: x : list of input vectors

Input: θ_0 : initial parameter vector

```

1:  $t \leftarrow 0$ 
2:  $s_{upd} \leftarrow 0$ 
3:  $g_t \leftarrow \vec{0}$ 
4: while  $\theta_t$  not converged do
5:    $l_0 \leftarrow L(x_t; \theta_t)$ 
6:    $d_t \leftarrow -\nabla_{\theta_t} L(x_t; \theta_t) + \beta d_{t-1}$ 
7:    $l_\mu \leftarrow L(x_t; \theta_t + \mu \frac{d_t}{\|d_t\|})$ 
8:    $b \leftarrow \nabla_{\theta_t} L(x_t; \theta_t) \cdot \frac{d_t}{\|d_t\|}$ 
9:    $a \leftarrow \frac{l_\mu - l_0 - b\mu}{\mu^2}$ 
10:  if  $a > 0$  and  $b < 0$  then
11:     $s_{upd} \leftarrow -\alpha \frac{b}{2a}$ 
12:  else if  $a \leq 0$  and  $b < 0$  then
13:     $s_{upd} \leftarrow \mu$ 
14:  else
15:     $s_{upd} \leftarrow 0$ 
16:  end if
17:  if  $s_{upd} > s_{max}$  then
18:     $s_{upd} \leftarrow s_{max}$ 
19:  end if
20:   $\theta_{t+1} \leftarrow \theta_t + s_{upd} \frac{-d_t}{\|d_t\|}$ 
21:   $t \leftarrow t + 1$ 
22: end while
23: return  $\theta_t$ 

```

fits. The normalization of the gradient to a length of 1 (equation 1) was chosen to have the measuring distance μ independent of the gradient size. The length of the gradient is irrelevant since only the direction of the gradient is required for parabolic approximation. Note that two network inferences are required to determine $l(0)$ and $l(\mu)$. Thus, *PAL* needs two forward passes and one backward pass through a network, whereas other first-order optimizers such as *SGD* [26] and *ADAM* [18] only need one pass of each type. Thus, *PAL* needs more time for one update step, as can be seen in Table 1. The memory required by *PAL* is similar to *SGD* with momentum, since only the last line direction has to be saved. Both of *PAL*'s forward passes must have identical random number initializations, otherwise L is not continuous and a parabolic approximation is not applicable.

2.2. Case discrimination of parabolic approximations

Since not all parabolic approximations are suitable for parameter update steps, the following cases are distinguished: (Note that $b = l'(0)$ and $a = 0.5l''(0)$)

1. $a > 0$ and $b < 0$: parabolic approximation has positive curvature and negative slope at $l(0)$. It has a minimum in line direction. Parameter update is done as described in Section 2.1.
2. $a \leq 0$ and $b < 0$: parabolic approximation has negative curvature and negative slope that has a maximum in negative line direction, or is a line with negative slope. In those cases a parabolic approximation is inappropriate. Since the second measured point has a lower loss as the first, s_{upt} is set to μ .
3. Since $b = -\|g_t\|$ cannot be greater than 0, the only case left is an extremum at the current position ($b = l'(0) = 0$). In this case, no weight update is performed. However, the loss function is changed by the next batch.

While cases 2 and 3 never appeared in our experiments with data augmentations, we encountered them when not using it.

2.3. Additional Features

In our experiments the following features have shown to increase *PAL*'s performance or stability:

Conjugate gradient: Instead of following the direction of the negative gradient we follow a conjugate direction d_t :

$$d_t = -\nabla_{\theta_t} L(x_t; \theta_t) + \beta d_{t-1} \quad d_0 = -\nabla_{\theta_0} L(x_0; \theta_0) \quad (3)$$

with $\beta \in [0, 1]$. Since we now use a conjugate direction, $l'(0)$ changes to:

$$l'(0) = \nabla_{\theta_t} L(x_t; \theta_t) \cdot \frac{d_t}{\|d_t\|} \quad (4)$$

This approach is used to find a more optimal search direction than the negative gradient. We tried the formulas of Fletcher-Reeves [10], Polak-Ribire [25], Hestenes-Stiefel [14] and Dai-Yuan [6] to determine a good β for each time step t . However, choosing a constant β of value 0.2 or 0.4 performs equally well. For a slight speedup one could approximate $l'(0)$ with $\|d_t\|$.

Update step adaptation: Our preliminary experiments revealed a systematic error of constantly approximating with slightly too narrow parabolas. Therefore, s_{upd} gets multiplied by a parameter $\alpha \geq 1$ (compare to equation 1).

Maximum step size: To hinder the algorithm from failing due to inaccurate parabolic approximations, we use a maximum step size s_{max} . The new update step is given by $\min(s_{upd}, s_{max})$. However most of our experiments with $s_{max} = 10$ never reached this step size and still performed well.

3. Convergence proof and further conclusions

This section provides a convergence proof based on the assumption that each intersection of the loss function is a one dimensional parabolic function. This assumption is a simplified adaption to our empirical results that lines in negative gradient direction are locally almost parabolic (see Section 1). For the following results we assume a basic *PAL* without the additional features introduced in Section 2.3. Proofs of all given theorems are given in Appendix A.

The loss function \mathcal{L} is generally defined as the average over a batch-wise loss function L : $\mathcal{L}(\mathbf{x} : \theta) : \mathbb{R}^n \rightarrow \mathbb{R}$, $\mathbf{x} \mapsto \frac{1}{n} \sum_{i=1}^n L(\mathbf{x}_i : \theta)$ with n being the amount of batches and x_i defining a batch. At first we show, under the condition of our assumption, that L is a parabolic function.

Theorem 1. *Given a k -times continuously differentiable function $f(\mathbf{x}) : \mathbb{R}^n \rightarrow \mathbb{R}$ and given that $\forall \mathbf{l}_n, \mathbf{d}_n \in \mathbb{R}^n : f(\mathbf{l}_n + \mathbf{d}_n s)$ has the form $s \mapsto as^2 + bs + c$ with $a > 0$ and $s, a, b, c \in \mathbb{R}$ (along every line, $f(\mathbf{x})$ is a convex parabolic function) then $f(\mathbf{x})$ has the form $f(\mathbf{x}) = c + \mathbf{r}^T \mathbf{x} + \mathbf{x}^T \mathbf{Q} \mathbf{x}$ ($f(\mathbf{x})$ is a n -dimensional parabola) with \mathbf{Q} being positive definite.*

Now we show that *PAL* converges on L :

Theorem 2. **PAL* converges on $f(\mathbf{x}) : \mathbb{R}^n \rightarrow \mathbb{R}$, $f(\mathbf{x}) = c + \mathbf{r}^T \mathbf{x} + \mathbf{x}^T \mathbf{Q} \mathbf{x}$ with $\mathbf{Q} \in \mathbb{R}^{n \times n}$ hermitian and positive definite.*

However, for $\mathcal{L}(\mathbf{x} : \theta)$, *PAL* has no convergence guarantee. Given two shifted one-dimensional parabolas, $ax^2 + bx + c$ and $a(x+d)^2 + b(x+d) + c$, which are presented to *PAL* alternately, *PAL* will always do an update step to the minimum of one of these but never to the minimum of

the average of both. But, by changing the training procedure and assuming that each L_i has the same \mathbf{Q} this can be fixed:

Theorem 3. *If $\mathcal{L}(\theta) : \mathbb{R}^n \rightarrow \mathbb{R} \theta \mapsto \mathcal{L}(\theta) = \frac{1}{n} \sum_{i=1}^n c_i + \mathbf{r}_i^T \theta + \theta^T \mathbf{Q}_i \theta$ and $c_i + \mathbf{r}_i^T \theta + \theta^T \mathbf{Q}_i \theta = L(\theta : \mathbf{x}_i)$ with n being number the of batches and \mathbf{x}_i defining a batch. (Each batch defines a parabola. $\mathcal{L}(\theta)$ is the mean of these parabolas) And $\forall i, j \in \mathbb{N} : \mathbf{Q}_i = \mathbf{Q}_j$ and \mathbf{Q}_i positive definite. Then $\arg \min_{\theta} \mathcal{L}(\theta) = \frac{1}{n} \sum_{i=1}^n \arg \min_{\theta} L(\theta)$ holds.*

The results mean that under our assumptions the location of the minimum of the loss function is given by the average of the locations of the minima of the loss functions of each batch. Due to the parabolic shape of those functions, the minima locations are found by *PAL*. As a result, in a noisy scenario where each batch defines a parabola with identical \mathbf{Q} , *PAL* converges.

4. Related Work

PAL is based on well-known methods such as line search, the non linear conjugate gradient method and quadratic approximation, which can be found in Numerical Optimization [16]. The idea of using quadratic approximations for line searches is known from [16] chapter 3.5 Recently multiple line search approaches have been published. *Gradient only line search GOLS-I* [17] and *probabilistic line search* [22] are considering the discontinuous stochastic loss function. Whereas the *SGD with Armijo line-search* [33] samples, like *PAL*, additional losses from the same batch. *GOLS-I* searches for a minimum on lines by looking for a sign change in the first directional derivative in direction of the search direction. *Probabilistic line search* finds minima on lines of a stochastic loss function by approximation it with a Gaussian process surrogate and using a probabilistic formulation of the Wolf conditions. The last two approaches show that they can optimize successfully on several machine learning problems and can compete against *SGD* without momentum. However, both works are lacking comprehensive comparison to other optimization approaches. The *SGD with Armijo line-search* is an optimized backtracking line search based on the Armijo condition, which shows competitive performance against multiple optimizers on several DNN tasks. Contrasting *PAL* it does not consider any local properties of the loss landscape. [5] goes in a similar direction as *PAL* by analyzing possible line search approximations for DNNs.

Considering the parabolic approximation property of *PAL* as a assumption over the shape of the loss function, it can be compared to multiple state-of-the-art approaches. Adaptive methods such as *SGD* with momentum [26] *ADAM*[18], *ADAGRAD*[8], *ADABOUND*[21], *AMSGRAD*[24] or *RM-*

SPROP [32] infer additional information from past gradients to adapt to the noise of the stochastic loss function and improve their update steps. Those methods use neither second derivatives nor assumptions about the shape of the loss functions. In contrast, second order optimizers such as *oLBFGS* [29], the approach of Botev et.al [3], *L-SRI* [23], *QUICKPROP* [9] and *S-LSRI* [2], generally assume that the loss function can be approximated locally by a parabola of the same dimension as the loss function. Thus, Newton’s method is used to perform an update step to the minimum of this parabola. In addition, methods exist that approximate the loss function in specific directions. The *L4* adaption scheme [27] approximates the loss function linearly in negative gradient direction, whereas our approach approximates the loss function parabolically in negative gradient direction. While all mentioned first order optimization methods, as well as *L4* and *PAL*, are suitable for time efficient optimization, Botev et.al and *QUICKPROP* fail to achieve good results quickly [23][3][4].

5. Evaluation

5.1. Experimental Design

We performed a comprehensive evaluation to show the performance of *PAL* on a variety of DNN optimization problems. Therefore, we tested *PAL* on 4 state-of-the-art or commonly used architectures on CIFAR-10 [19], CIFAR100 [19] and IMAGENET [7]. For CIFAR10 we evaluated on DenseNet40s [15], EfficientNetB0s [31], ResNet32s [13] and MobileNetV2s [28]. For CIFAR100 we compared on the same networks except of using DenseNet100s instead of a DenseNet40s. On IMAGENET we evaluated on DenseNet121s, EfficientNetB0s, ResNet101s. The optimizers we compared *PAL* to are: *SGD* with momentum [26], *ADAM*[18], *RMSPROP*[32] and the recently published *RADAM*[20].

To perform a fair comparison we compared hyperparameter combinations from commonly used hyperparameters for each optimizer. In addition, we utilize those combinations, to analyze the hyperparameter sensitivity for each optimizer. Detailed lists of hyperparameters and data aug-

mentations used are given in Appendix C. For each hyperparameter combination we averaged our results over 3 runs using the seeds 1, 2 and 3. All in all we trained 1953 networks with Tensorflow 1.13 [1] on Nvidia Geforce GTX 1080 TI graphic cards. On CIFAR-10 and CIFAR-100 we trained between 1 and 2 hours, depending on the network. On IMAGENET each network was trained for 48 hours.

The training set to evaluation set split was 45000 to 15000 for CIFAR10 and CIFAR100. At the time of writing the default Tensorflow classes do not support the reuse of the same randomly sampled numbers for multiple inferences, therefore we implemented and used our own Dropout [30] layer.

To get a fair comparison of the optimizers capabilities we compared on the training loss, the evaluation loss and the test accuracy metrics. For all metrics we provide the median and the quartiles to analyze the hyperparameter sensitivity.

Much work has been done in recent years to find effective learning rate schedules for learning rate based optimizers. However, for *PAL*, the concept of a learning rate is missing. It would exceed the scope of this paper to analyze perfect hyperparameter schedules for *PAL*. Therefore, we compared the optimizers in their published form and did not apply any decay or further improving mechanisms.

5.2. Comparison on training steps

To analyze whether *PAL*’s training steps are more effective we plotted the training loss over the training steps for the best runs of EfficientNet and MobileNetV2 on CIFAR10 and CIFAR100. The results are given in Figure 4. One can see that *PAL* reaches significant lower training loss for all compared scenarios in less training steps. This means that, *PAL*’s training steps are more effective than those of the other optimizers.

5.3. Comparison on wall clock time

It is a commonly used approach to compare optimizer performance in training steps [21],[18], [8]. However, a comparison of training steps is not appropriate in this scenario. Considering Table 1, which shows the amount of

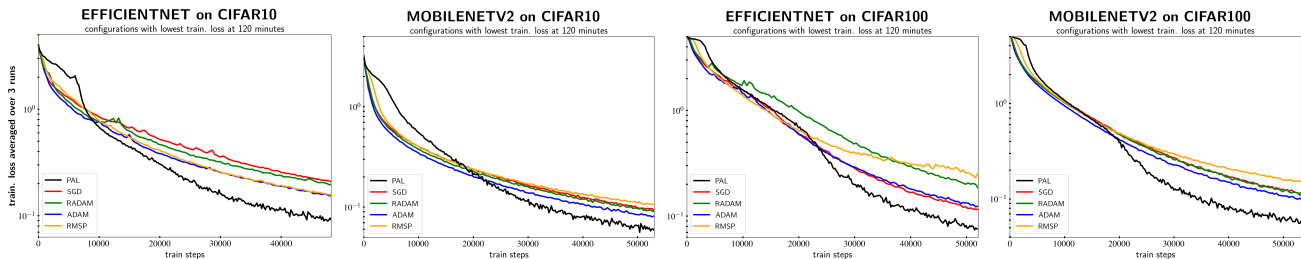


Figure 4: Comparison of *PAL* to *SGD*, *RADAM*, *ADAM* and *RMSPROP* on the best training loss curves. Considering training steps, our approach outperforms the others.

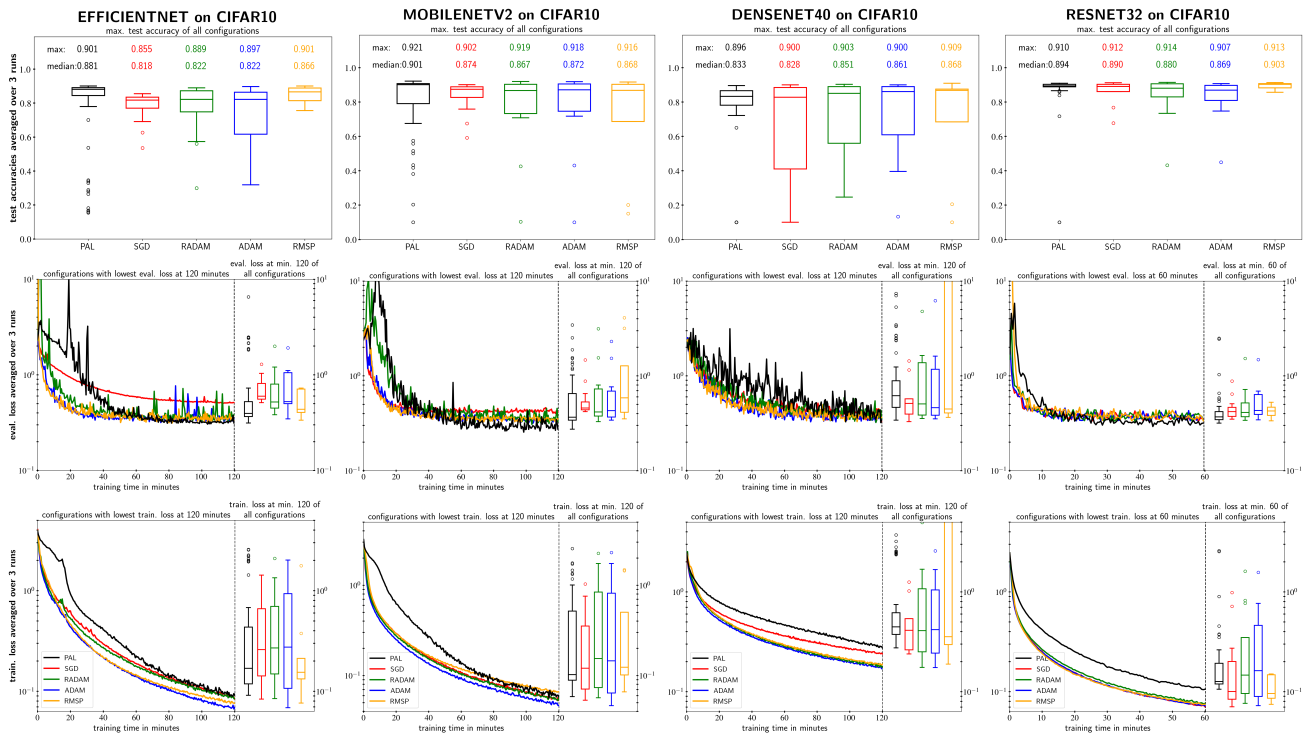


Figure 5: Wall clock time comparison on **CIFAR10** of *PAL*, *SGD*, *RADAM*, *ADAM*, *RMSPROP* on test accuracy, eval. loss and train. loss. Results are averaged over 3 runs. Box plots result from comprehensive hyperparameter grid searches in plausible intervals. *PAL* competes against the other optimizers on test accuracy and evaluation loss

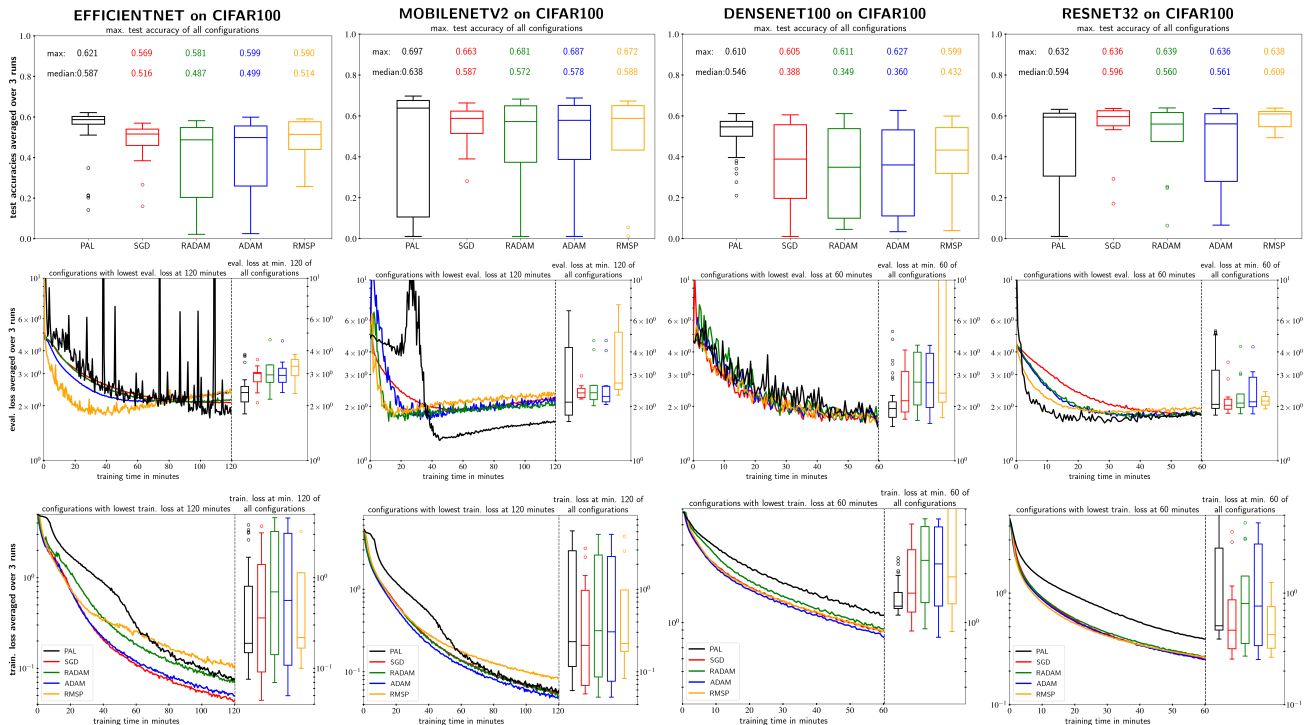


Figure 6: Wall clock time comparison identical to the description of Figure 5 but performed on **CIFAR100**. *PAL* can outperform the other optimizers on test accuracy and evaluation loss on EfficientNet and MobileNet

Table 1: Example comparison of the number of epochs trained on CIFAR10 of *PAL* and *SGD* with momentum in the given training times. *ADAM*, *RMSP* and *RADAM* reach a similar amount of epochs as *SGD*. Although *PAL* is slower, it can compete with the other optimizers by performing more efficient update steps.

network	training time	epochs <i>PAL</i>	epochs <i>SGD</i>	% <i>PAL</i> of <i>SGD</i>
ResNet32	60 min	128.8	302.0	42.6%
MobilenetV2	120 min	117.9	206.4	57.2%
EfficientNet	120 min	107.2	234.7	45.7%
DenseNet40	120 min	72.0	116.8	61.0%

epochs *PAL* performs in a specific time compared to *SGD*, it can be seen that *PAL* is up to a factor of 0.426 slower than *SGD*. Therefore, although it is detrimental to our approach, we decided to perform a fair wall-clock time comparison of the training processes. A second detrimental issue is that we compare the basic Tensorflow implementations of *PAL* against on CUDA level optimized Tensorflow implementations of *ADAM*, *SGD* and *RMSP*.

Figure 5 shows the result of our comparison on CIFAR10. For EfficientNet and MobileNet lower evaluation losses and higher test accuracies can be reached with *PAL*. As expected, the training loss of the best runs is decaying slower for *PAL* than for the other optimizers. However, the median training loss is lower for three out of four networks. This means that *PAL* is generalizing better in the given scenarios since the overfitting effect is not that strong. In addition,

the results show that the hyperparameter sensitivity for all metrics depends strongly on the network. We cannot see a trend that one optimizer is in general less hyperparameter sensitive than the others. In general *SGD* with momentum performs worst, whereas all other optimizers perform on the same level. The fact that the final training losses of *PAL* applied on MobilenetV2 and EfficientNet can compete, although the other optimizers are of a factor 1.75 and 2.22 faster, emphasizes the efficiency of *PAL*'s update steps. Similar results are found in our experiments on CIFAR100 (see Figure 6). However, in this scenario *PAL* can reach significantly better results on test accuracy and evaluation loss on EfficientNet and MobileNet than the other optimizers. Considering the median the evaluation loss is also lower on a DenseNet100. In addition, the evaluation loss on a ResNet32 decreases much faster than for the other optimizers in the best run. In addition, the best training loss curve of MobilenetV2 can compete, although *PAL* is a factor 0.57 slower. Considering the median it can even compete on all networks. In contrast to the evaluation on CIFAR10, *SGD* performs on the same level than the other optimizers in this scenario.

We also compared all optimizers to a simple RNN trained on a letter prediction task on the TOLSTOI WAR AND PEACE dataset Figure 7 column 1. All optimizers show almost equal performance. The hyperparameter sensitivity of *RMSP* is quite low, which is consistent with its common usage for RNN tasks.

Since training on IMAGENET is expensive, we tested only the 3 best hyperparameter combinations found in our evaluation on CIFAR100. Therefore, those results have to be

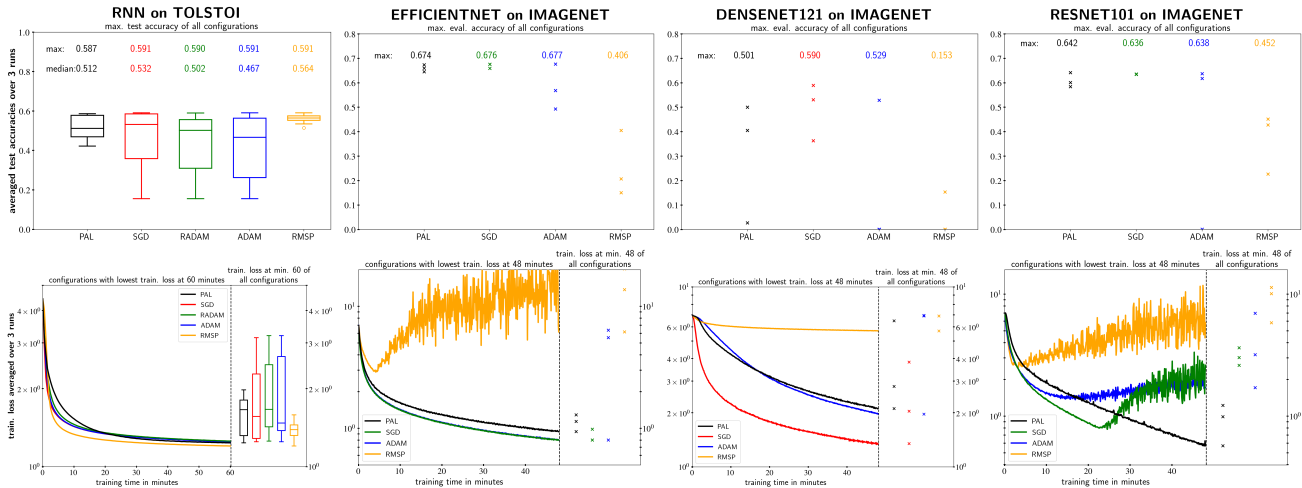


Figure 7: Comparison of *PAL* to *SGD*, *RADAM*, *ADAM*, *RMSPROP* on test accuracy, eval. loss and train. loss. on **IMAGENET**, and a simple RNN, trained on the **TOLSTOI** dataset. For IMAGENET the best 3 hyperparameter configuration from the CIFAR100 evaluation were used. These unusual results are likely owed to the justified omission of learning rate schedules (see Section 5.1). Evaluation loss plots were omitted since they showed nothing of interest.

handled with care, since different hyperparameters might lead to significantly different results. However, those results give an intuition in how far hyperparameters can be reused over different datasets. We also skipped the evaluation with *RADAM* since it had consistently similar results to *ADAM* on previous evaluations. Our results are presented in Figure 7 column 2-4. For *PAL SGD* and *ADAM* at least some of the hyperparameters for CIFAR100 can again achieve good results on IMAGENET. However, *RMSP* tends to diverge. On a ResNetT101 *PAL* is the only optimizer than can perform well. The loss of all other optimizers is increasing after some time. These unusual results are likely owed to the justified omission of learning rate schedules (see Section 5.1).

One additional result of our evaluation is that the conjugate gradient feature, which can be seen as a moving average over the negative gradient direction, can increase the performance, but only slightly. This means, that our approach works well although ignoring the noise of the stochastic loss function completely.

After analyzing the best hyper parameter combinations of *PAL* over all experiments, we suggest to use values from the following parameter intervals:

$$\mu = [0.1, 1], \alpha = [1.2, 1.6], \beta = [0, 0.4], s_{max} = [1, 10].$$

A table with exact numerical results of all experiments is provided in Appendix B.

6. Conclusions & Discussion

With our batchwise parabolic approximation line search (*PAL*) we present an efficient line search variant for deep neural networks, based on the combination of multiple well known methods such as parabolic approximations, conjugate gradients and line searches. In Figure 2 we show empirically, by considering the angle between the search direction and the gradient at the assumed minimum, that parabolic approximations are well suited to approximate lines of the considered loss functions. This property holds for several common used or state-of-the-art networks trained on CIFAR10. Since *PAL* performs also well on CIFAR100 and IMAGENET, it is plausible that this property holds on those, too. The fact that parabolic approximations fits well for DNN optimization processes softens the general view of deep learning loss functions as being highly non convex.

Our comprehensive evaluation, including state-of-the-art or common used optimizers trained on several hyperparameter combinations, architectures and datasets, shows that *PAL* outperforms other optimizers on a training-step wise scale, by performing more effective update steps. However, we also show that *PAL* is up to a factor of 0.43 slower than other optimizers. Thus, we performed an uncommon but fair wall-clock comparison of the training processes. This is obviously detrimental for our approach since firstly we

need longer per update step and secondly we compare our basic tensorflow implementations of *PAL* against on CUDA level tensorflow implementations. Unexpectedly, our optimizer tends to generalize better than the other optimizers, since *PAL* cannot compete with other optimizers on the lowest training loss, but it can compete and sometimes even outperform other optimizers on evaluation loss and test accuracy.

On a theoretical basis we prove that *PAL* converges on n-dimensional discrete parabolic functions. However, we also argued that there is no convergence guarantee on n-dimensional stochastic parabolic functions. Although these proofs provide some important first steps for a theoretical foundation of the algorithm, they are of less importance in practice, since we could show empirically that our approach decreases the loss effectively.

The interesting result of this work is that, in contrast to common optimizers, we are ignoring the noise origination from batch sampling of the loss function completely by assuming, that the minimum of a line in negative gradient direction from one batch sample is a good estimator for the real minimum in line direction. However, measuring the real minimum of a line of discontinuous stochastic loss function is, in combination with data augmentation and large datasets, virtually impossible, especially, if this should be done for multiple lines. Nevertheless, the prominent training-step-wise performance of our optimizer, provides evidence that our assumption holds.

7. Outlook

Our future work will be focused on taking the noise theoretically and empirically into account. Firstly we are going to analyze whether one of the existing optimization approaches can be combined reasonably with our approach. Secondly we are going to analyze, whether lines of discontinuous stochastic loss functions can also be approximated by simple functions, and how many measurements are needed, to fit those approximations. As a part of this approach, we are planing to sample the distributions of loss values at multiple consecutive line positions for low data machine learning problems.

References

- [1] Martín Abadi, Ashish Agarwal, Paul Barham, Eugene Brevdo, Zhifeng Chen, Craig Citro, Greg S. Corrado, Andy Davis, Jeffrey Dean, Matthieu Devin, Sanjay Ghemawat, Ian Goodfellow, Andrew Harp, Geoffrey Irving, Michael Isard, Yangqing Jia, Rafal Jozefowicz, Lukasz Kaiser, Manjunath Kudlur, Josh Levenberg, Dandelion Mané, Rajat Monga, Sherry Moore, Derek Murray, Chris Olah, Mike Schuster, Jonathon Shlens, Benoit Steiner, Ilya Sutskever, Kunal Talwar, Paul Tucker, Vincent Vanhoucke, Vijay Vasudevan, Fernanda Viégas, Oriol Vinyals, Pete Warden, Martin Wattenberg, Martin Wicke, Yuan Yu, and Xiaoqiang Zheng. TensorFlow: Large-scale machine learning on heterogeneous systems, 2015. Software available from tensorflow.org.
- [2] Albert S. Berahas, Majid Jahani, and Martin Takáč. Quasi-newton methods for deep learning: Forget the past, just sample. *CoRR*, abs/1901.09997, 2019.
- [3] Aleksandar Botev, Hippolyt Ritter, and David Barber. Practical gauss-newton optimisation for deep learning. *arXiv preprint arXiv:1706.03662*, 2017.
- [4] Clemens-Alexander Brust, Sven Sickert, Marcel Simon, Erik Rodner, and Joachim Denzler. Neither quick nor proper - evaluation of quickprop for learning deep neural networks. *CoRR*, abs/1606.04333, 2016.
- [5] Younghwan Chae and Daniel N Wilke. Empirical study towards understanding line search approximations for training neural networks. *arXiv preprint arXiv:1909.06893*, 2019.
- [6] Yu-Hong Dai and Yaxiang Yuan. A nonlinear conjugate gradient method with a strong global convergence property. *SIAM Journal on optimization*, 10(1):177–182, 1999.
- [7] J. Deng, W. Dong, R. Socher, L.-J. Li, K. Li, and L. Fei-Fei. ImageNet: A Large-Scale Hierarchical Image Database. In *CVPR09*, 2009.
- [8] John Duchi, Elad Hazan, and Yoram Singer. Adaptive sub-gradient methods for on learning and stochastic optimization. *Journal of Machine Learning Research*, 12(Jul):2121–2159, 2011.
- [9] Scott E Fahlman et al. An empirical study of learning speed in back-propagation networks. 1988.
- [10] Reeves Fletcher and Colin M Reeves. Function minimization by conjugate gradients. *The computer journal*, 7(2):149–154, 1964.
- [11] Ian J Goodfellow, Oriol Vinyals, and Andrew M Saxe. Qualitatively characterizing neural network optimization problems. *arXiv preprint arXiv:1412.6544*, 2014.
- [12] Google. Tensorflow adam optimizer documentation. https://www.tensorflow.org/api_docs/python/tf/train/AdamOptimizer. Accessed: 2019-11-12.
- [13] Kaiming He, Xiangyu Zhang, Shaoqing Ren, and Jian Sun. Deep residual learning for image recognition. In *Proceedings of the IEEE conference on computer vision and pattern recognition*, pages 770–778, 2016.
- [14] Magnus Rudolph Hestenes and Eduard Stiefel. *Methods of conjugate gradients for solving linear systems*, volume 49. NBS Washington, DC, 1952.
- [15] Gao Huang, Zhuang Liu, Laurens Van Der Maaten, and Kilian Q Weinberger. Densely connected convolutional networks. In *CVPR*, volume 1, page 3, 2017.
- [16] Stephen Wright Jorge Nocedal. *Numerical Optimization*. Springer series in operations research. Springer, 2nd ed edition, 2006.
- [17] Dominic Kafka and Daniel Wilke. Gradient-only line searches: An alternative to probabilistic line searches. *arXiv preprint arXiv:1903.09383*, 2019.
- [18] Diederik P. Kingma and Jimmy Ba. Adam: A method for stochastic optimization. *CoRR*, abs/1412.6980, 2014.
- [19] Alex Krizhevsky and Geoffrey Hinton. Learning multiple layers of features from tiny images. Technical report, Cite-seer, 2009.
- [20] Liyuan Liu, Haoming Jiang, Pengcheng He, Weizhu Chen, Xiaodong Liu, Jianfeng Gao, and Jiawei Han. On the variance of the adaptive learning rate and beyond, 2019.
- [21] Liangchen Luo, Yuanhao Xiong, and Yan Liu. Adaptive gradient methods with dynamic bound of learning rate. In *International Conference on Learning Representations*, 2019.
- [22] Maren Mahsereci and Philipp Hennig. Probabilistic line searches for stochastic optimization. *Journal of Machine Learning Research*, 18, 2017.
- [23] Vivek Ramamurthy and Nigel Duffy. L-sr1: a second order optimization method. 2017.
- [24] Sashank J. Reddi, Satyen Kale, and Sanjiv Kumar. On the convergence of adam and beyond. In *International Conference on Learning Representations*, 2018.
- [25] G Ribière and E Polak. Note sur la convergence de directions conjuguées. *Rev. Francaise Informat Recherche Opertionelle*, 16:35–43, 1969.
- [26] H. Robbins and S. Monro. A stochastic approximation method. *Annals of Mathematical Statistics*, 22:400–407, 1951.
- [27] Michal Rolinek and Georg Martius. L4: Practical loss-based stepsize adaptation for deep learning. In *Advances in Neural Information Processing Systems*, pages 6434–6444, 2018.
- [28] Mark Sandler, Andrew G. Howard, Menglong Zhu, Andrey Zhmoginov, and Liang-Chieh Chen. Mobilenetv2: Inverted residuals and linear bottlenecks. *2018 IEEE/CVF Conference on Computer Vision and Pattern Recognition*, pages 4510–4520, 2018.
- [29] Nicol N. Schraudolph, Jin Yu, and Simon Gnter. A stochastic quasi-newton method for online convex optimization. In Marina Meila and Xiaotong Shen, editors, *Proceedings of the Eleventh International Conference on Artificial Intelligence and Statistics*, volume 2 of *Proceedings of Machine Learning Research*, pages 436–443, San Juan, Puerto Rico, 21–24 Mar 2007. PMLR.
- [30] Nitish Srivastava, Geoffrey Hinton, Alex Krizhevsky, Ilya Sutskever, and Ruslan Salakhutdinov. Dropout: A simple way to prevent neural networks from overfitting. *Journal of Machine Learning Research*, 15:1929–1958, 2014.
- [31] Mingxing Tan and Quoc V. Le. Efficientnet: Rethinking model scaling for convolutional neural networks. In *ICML*, 2019.

- [32] Tijmen Tieleman and Geoffrey Hinton. Lecture 6.5-rmsprop, coursera: Neural networks for machine learning. *University of Toronto, Technical Report*, 2012.
- [33] Sharan Vaswani, Aaron Mishkin, Issam Laradji, Mark Schmidt, Gauthier Gidel, and Simon Lacoste-Julien. Painless stochastic gradient: Interpolation, line-search, and convergence rates. *arXiv preprint arXiv:1905.09997*, 2019.

A. Proofs

Theorem 1. Given a k -times continuously differentiable function $f(\mathbf{x}) : \mathbb{R}^n \rightarrow \mathbb{R}$ and given that $\forall \mathbf{l}_n, \mathbf{d}_n \in \mathbb{R}^n : f(\mathbf{l}_n + \mathbf{d}_n s) = as^2 + bs + c$ for some $a, b, c \in \mathbb{R}$ with $a > 0$ (along every line, $f(\mathbf{x})$ is a convex parabolic function) then $f(\mathbf{x})$ has the form $f(\mathbf{x}) = c + \mathbf{r}^T \mathbf{x} + \mathbf{x}^T \mathbf{Q} \mathbf{x}$ for some $\mathbf{r} \in \mathbb{R}^n$ and $\mathbf{Q} \in \mathbb{R}^{n \times n}$ ($f(\mathbf{x})$ is a n -dimensional parabola) with \mathbf{Q} being positive definite.

Proof.

$$g(\mathbf{x}) = u + \mathbf{v}^T \mathbf{x} + \mathbf{x}^T \mathbf{W} \mathbf{x} \text{ for some } u \in \mathbb{R}, \mathbf{v} \in \mathbb{R}^n \text{ and } \mathbf{W} \in \mathbb{R}^{n \times n}$$

$$\Leftrightarrow \forall \mathbf{l}_n, \mathbf{d}_n \in \mathbb{R}^n \wedge \|\mathbf{d}_n\| = 1 : \sum_{j=1}^n \sum_{k=1}^n \sum_{l=1}^n \frac{\partial^3 g(\mathbf{l}_n)}{\partial x_j \partial x_k \partial x_l} d_{n_j} d_{n_k} d_{n_l} = 0 \quad (5)$$

\Rightarrow holds since we have a polynomial of degree 2 and its third derivative is always a $\mathbf{0}$ tensor.

\Leftarrow holds since the remainder of the quadratic Taylor expansion is always 0.

In our case the right part is 0 since:

$$\sum_{j=1}^n \sum_{k=1}^n \sum_{l=1}^n \frac{\partial^3 f(\mathbf{l}_n)}{\partial x_j \partial x_k \partial x_l} d_{n_j} d_{n_k} d_{n_l} = \frac{\partial}{\partial s^3} f(\mathbf{l}_n + \mathbf{d}_n s) = 0 \quad (6)$$

In words: $f(\mathbf{x})$ is a parabolic function if and only if for each location \mathbf{l}_n the third directional derivative of $f(\mathbf{l}_n)$ in each direction \mathbf{d}_n is 0. Which is the case, since the third derivative of each intersection is 0.

\mathbf{W} is positive definite since:

$$\forall \mathbf{d}_n, \mathbf{l}_n \in \mathbb{R}^n \wedge \|\mathbf{d}_n\| = 1 : \mathbf{d}_n^T \mathbf{W} \mathbf{d}_n = \frac{1}{2} \mathbf{d}_n^T \mathbf{H}(\mathbf{l}_n) \mathbf{d}_n = \frac{1}{2} \frac{\partial}{\partial s^2} f(\mathbf{l}_n + \mathbf{d}_n s) = a > 0 \quad (7)$$

■

Theorem 2. PAL converges on $f(\mathbf{x}) : \mathbb{R}^n \rightarrow \mathbb{R}, f(\mathbf{x}) = c + \mathbf{r}^T \mathbf{x} + \mathbf{x}^T \mathbf{Q} \mathbf{x}$ with $\mathbf{Q} \in \mathbb{R}^{n \times n}$ hermitian and positive definite.

Proof.

For this prove we consider a basic PAL without the features introduced in Section 2.3. Note, that during the proof we will see, that $a > 0$ and $b < 0$. Thus, only the update step for this case has to be considered (see Section 2.2).

$f(\mathbf{x})$ is convex since \mathbf{Q} is positive definite. Thus it has one minimum.

Without loss of generality we set $c = 0, \mathbf{r} = \mathbf{0}, \mathbf{x}_n \neq 0$

$$f(\mathbf{x}) = \mathbf{x}^T \mathbf{Q} \mathbf{x} \text{ and } \nabla_{\mathbf{x}} f(\mathbf{x}) = f'(\mathbf{x}) = 2\mathbf{Q} \mathbf{x} \quad (8)$$

The values of $f(x)$ along a line through \mathbf{x} in the direction of $-f'(\mathbf{x})$ are given by:

$$f(-f'(\mathbf{x})\hat{s} + \mathbf{x}) \quad (9)$$

We expand the line function:

$$\begin{aligned} f(-f'(\mathbf{x})\hat{s} + \mathbf{x}) &= f(-2\mathbf{Q}\mathbf{x}\hat{s} + \mathbf{x}) \\ &= (-2\mathbf{Q}\mathbf{x}\hat{s} + \mathbf{x})^T \mathbf{Q} (-2\mathbf{Q}\mathbf{x}\hat{s} + \mathbf{x}) \\ &= \underbrace{4\mathbf{x}^T \mathbf{Q}^3 \mathbf{x}}_{=:a} \hat{s}^2 + \underbrace{-4\mathbf{x}^T \mathbf{Q}^2 \mathbf{x}}_{=:b} \hat{s} + \underbrace{\mathbf{x}^T \mathbf{Q} \mathbf{x}}_{=:c} \end{aligned} \quad (10)$$

Here we see that $f(\hat{s})$ is indeed a parabolic function with $a > 0, b < 0$ and $c > 0$ since $\mathbf{Q}^3, \mathbf{Q}^2$ and \mathbf{Q} are positive definite. The location of the minimum s_{min} of $f(\hat{s})$ is given by:

$$\hat{s}_{min} = \arg \min_{\hat{s}} f(-f'(\mathbf{x})\hat{s} + \mathbf{x}) = -\frac{b}{2a} \quad (11)$$

PAL determines \hat{s}_{min} exactly with $\hat{s}_{min} = \frac{s_{upd}}{\|f'(x)\|}$ (see equation 1 and 2). $\|f'(x)\| > 0$ since otherwise we would already be in the minimum.

The value at the minimum is given by:

$$f(\hat{s}_{min}) = a\left(\frac{-b}{2a}\right)^2 + b\left(\frac{-b}{2a}\right) + c = -\frac{b^2}{4a} + c = -\underbrace{\frac{(-\mathbf{x}^T \mathbf{Q}^2 \mathbf{x})^2}{\mathbf{x}^T \mathbf{Q}^3 \mathbf{x}}}_{=:g(\mathbf{x})} + \mathbf{x}^T \mathbf{Q} \mathbf{x} = -g(\mathbf{x}) + f(\mathbf{x}) \quad (12)$$

Since \mathbf{Q}^2 and \mathbf{Q}^3 are positive definite and $\mathbf{x} \neq 0$:

$$g(\mathbf{x}) > 0 \quad (13)$$

Now we consider the sequence $f(\mathbf{x}_n)$, with \mathbf{x}_n defined by *PAL* (see Equation 1):

$$\mathbf{x}_{n+1} = -\frac{f'(\mathbf{x}_n)}{\|f'(\mathbf{x}_n)\|} \hat{s}_{upd} + \mathbf{x}_n = -f'(\mathbf{x}_n) \hat{s}_{min} + \mathbf{x}_n \quad (14)$$

It is easily seen by induction that:

$$0 < f(\mathbf{x}_{n+1}) < f(\mathbf{x}_n) = \sum_{i=0}^{n-1} -g(\mathbf{x}_i) + f(\mathbf{x}_0) < f(\mathbf{x}_0). \quad (15)$$

$g(\mathbf{x}_n)$ converges to 0. Since $\forall n : g(\mathbf{x}_n) > 0$ and $\sum_{i=0}^{n-1} -g(\mathbf{x}_i)$ is bounded.

Now we have to show that \mathbf{x}_n converges to 0.

We have:

$$g(\mathbf{x}_n) = \frac{(\mathbf{x}_n^T \mathbf{Q}^2 \mathbf{x}_n)^2}{\mathbf{x}_n^T \mathbf{Q}^3 \mathbf{x}_n} = \frac{\langle \mathbf{x}_n, \mathbf{Q}^2 \mathbf{x}_n \rangle^2}{\langle \mathbf{x}_n, \mathbf{Q}^3 \mathbf{x}_n \rangle} \quad (16)$$

Now we use the theorem of Courant-Fischer:

$$\langle x, x \rangle \min\{\lambda_1, \dots, \lambda_n\} \leq \langle x, Ax \rangle \leq \langle x, x \rangle \max\{\lambda_1, \dots, \lambda_n\} \text{ for any symmetric } A \in \mathbb{R}^{n \times n} \text{ with } \lambda_1, \dots, \lambda_n \quad (17)$$

And get:

$$g(\mathbf{x}_n) \geq \frac{\lambda_{\mathbf{Q}^2 \min}^2 \langle \mathbf{x}_n, \mathbf{x}_n \rangle^2}{\lambda_{\mathbf{Q}^3 \max} \langle \mathbf{x}_n, \mathbf{x}_n \rangle} = C \frac{\|\mathbf{x}_n\|^4}{\|\mathbf{x}_n\|^2} = C \|\mathbf{x}_n\|^2 \quad (18)$$

with

$$C = \frac{\lambda_{\mathbf{Q}^2 \min}^2}{\lambda_{\mathbf{Q}^3 \max}} > 0 \text{ since all } \lambda \text{ of the positive definite } \mathbf{Q} \text{ are positive} \quad (19)$$

Thus we have:

$$g(\mathbf{x}_n) \geq C \|\mathbf{x}_n\|^2 \geq 0 \quad (20)$$

Since $g(\mathbf{x}_n)$ converges to 0, $C \|\mathbf{x}_n\|^2$ converges to 0.

This means \mathbf{x}_n converges to $\mathbf{0}$, which is the location of the minimum. ■

Theorem 3. If $\mathcal{L}(\theta) : \mathbb{R}^n \rightarrow \mathbb{R}$ $\theta \mapsto \mathcal{L}(\theta) = \frac{1}{n} \sum_{i=1}^n L(\theta : \mathbf{x}_i)$ with $L(\theta : \mathbf{x}_i) = c_i + \mathbf{r}_i^T \theta + \theta^T \mathbf{Q}_i \theta$. n is the number of batches and \mathbf{x}_i defines a batch. c_i , \mathbf{r}_i and \mathbf{Q}_i depend on \mathbf{x}_i . And $\forall i, j \in \mathbb{N} : \mathbf{Q}_i = \mathbf{Q}_j$ and \mathbf{Q}_i positive definite. (Each batch is defining a parabola with identical \mathbf{Q} . $\mathcal{L}(\theta)$ is the mean of these parabolas). Then $\arg \min_{\theta} \mathcal{L}(\theta) = \frac{1}{n} \sum_{i=1}^n \arg \min_{\theta} L(\theta)$ holds.

Proof.

Since $\mathcal{L}(\theta)$ is a sum of convex functions, it is also convex and has one minimum.

At first we determine the derivative of $\mathcal{L}(\theta)$ with respect to θ :

$$\frac{\partial}{\partial \theta} \mathcal{L}(\theta) = \frac{1}{n} \sum_{i=1}^n (\mathbf{r}_i + 2\mathbf{Q}_i \theta) = 2\mathbf{Q}\theta + \frac{1}{n} \sum_{i=1}^n \mathbf{r}_i \quad (21)$$

Then we determine the minima:

$$\arg \min_{\theta} \mathcal{L}(\theta) \Leftrightarrow \frac{\partial}{\partial \theta} \mathcal{L}(\theta) = 0 \Leftrightarrow \theta = -\frac{1}{2} \left(\sum_{i=1}^n \mathbf{Q}_i \right)^{-1} \sum_{i=1}^n \mathbf{r}_i = -\frac{1}{2n} \mathbf{Q}^{-1} \sum_{i=1}^n \mathbf{r}_i \quad (22)$$

$$\arg \min_{\mathbf{t}} L(\mathbf{t} : \mathbf{x}_i) = -\frac{1}{2} \mathbf{Q}^{-1} \mathbf{r}_i \quad (23)$$

Thus, we get:

$$\arg \min_{\theta} \mathcal{L}(\theta) = -\frac{1}{2n} \mathbf{Q}^{-1} \sum_{i=1}^n \mathbf{r}_i = \frac{1}{n} \sum_{i=1}^n -\frac{1}{2} \mathbf{Q}^{-1} \mathbf{r}_i = \frac{1}{n} \sum_{i=1}^n \arg \min_{\mathbf{t}} L(\mathbf{t} : \mathbf{x}_i) \quad (24)$$

■

B. Detailed experimental results

See table 2 on the next page.

Table 2: Performance comparison of *PAL RMSPROP*, *ADAM*, *RADAM* and *SGD*. All hyperparameter combinations given in Appendix C were evaluated for each architecture. Results are averaged over 3 runs starting from different random seeds, except for training on ImageNet, for which results were not averaged.

dataset	network	optimizer	training loss		evaluation accuracy		test accuracy	
			min	median; p25; p75	max	median; p25; p75	max	median; p25; p75
CIFAR10	EFFICIENTNET	RMSP	0.076	0.154 ; 0.133; 0.213	0.912	0.885; 0.824; 0.902	0.901	0.866; 0.814; 0.889
		ADAM	0.069	0.275; 0.107; 0.934	0.911	0.836; 0.772; 0.879	0.897	0.822; 0.617; 0.864
		RADAM	0.085	0.27; 0.149; 0.697	0.907	0.838; 0.758; 0.888	0.889	0.822; 0.748; 0.872
		SGD	0.084	0.26; 0.142; 0.661	0.864	0.829; 0.787; 0.851	0.855	0.818; 0.77; 0.835
		PAL	0.091	0.169; 0.119; 0.435	0.914	0.9 ; 0.873; 0.906	0.901	0.881 ; 0.845; 0.891
CIFAR10	MOBILENETV2	RMSP	0.066	0.124; 0.101; 0.503	0.924	0.883; 0.744; 0.915	0.916	0.868; 0.687; 0.903
		ADAM	0.046	0.145; 0.064; 0.815	0.926	0.884; 0.757; 0.916	0.918	0.872; 0.747; 0.905
		RADAM	0.057	0.154; 0.074; 0.841	0.925	0.883; 0.747; 0.914	0.919	0.867; 0.733; 0.903
		SGD	0.053	0.121; 0.071; 0.353	0.914	0.885; 0.851; 0.901	0.902	0.874; 0.827; 0.889
		PAL	0.058	0.102 ; 0.089; 0.518	0.936	0.916 ; 0.819; 0.921	0.921	0.901 ; 0.79; 0.908
CIFAR10	DENSENET40	RMSP	0.189	0.356 ; 0.296; 26.545	0.913	0.879 ; 0.709; 0.887	0.909	0.868 ; 0.684; 0.875
		ADAM	0.174	0.419; 0.244; 1.046	0.916	0.87; 0.626; 0.899	0.9	0.861; 0.609; 0.89
		RADAM	0.175	0.41; 0.251; 1.074	0.918	0.866; 0.595; 0.904	0.903	0.851; 0.56; 0.89
		SGD	0.239	0.413; 0.263; 0.54	0.908	0.838; 0.413; 0.897	0.9	0.828; 0.411; 0.885
		PAL	0.275	0.446; 0.375; 0.618	0.904	0.872; 0.858; 0.89	0.896	0.833; 0.782; 0.866
CIFAR10	RESNET32	RMSP	0.075	0.096 ; 0.086; 0.148	0.923	0.913 ; 0.895; 0.916	0.913	0.903 ; 0.883; 0.907
		ADAM	0.072	0.163; 0.09; 0.461	0.917	0.879; 0.841; 0.909	0.907	0.869; 0.81; 0.897
		RADAM	0.076	0.147; 0.096; 0.35	0.922	0.896; 0.846; 0.915	0.914	0.88; 0.83; 0.907
		SGD	0.071	0.1; 0.084; 0.201	0.92	0.909; 0.875; 0.913	0.912	0.89; 0.861; 0.903
		PAL	0.106	0.127; 0.119; 0.193	0.921	0.911; 0.907; 0.915	0.91	0.894; 0.888; 0.903
CIFAR100	DENSENET100	RMSP	0.881	1.908; 1.305; 263.042	0.614	0.449; 0.334; 0.572	0.599	0.432; 0.319; 0.543
		ADAM	0.813	2.295; 1.265; 3.872	0.621	0.364; 0.106; 0.54	0.627	0.36; 0.11; 0.531
		RADAM	0.915	2.416; 1.326; 3.892	0.608	0.349; 0.097; 0.535	0.611	0.349; 0.099; 0.537
		SGD	0.887	1.516; 1.16; 2.805	0.609	0.397; 0.2; 0.565	0.605	0.388; 0.196; 0.556
		PAL	1.111	1.263 ; 1.222; 1.533	0.605	0.57 ; 0.536; 0.583	0.61	0.546 ; 0.5; 0.573
CIFAR100	EFFICIENTNET	RMSP	0.1	0.219; 0.167; 1.133	0.591	0.514; 0.448; 0.577	0.59	0.514; 0.439; 0.576
		ADAM	0.05	0.56; 0.108; 3.075	0.596	0.491; 0.297; 0.554	0.599	0.499; 0.259; 0.555
		RADAM	0.07	0.695; 0.141; 3.221	0.585	0.487; 0.233; 0.55	0.581	0.487; 0.203; 0.548
		SGD	0.044	0.359; 0.091; 1.398	0.568	0.513; 0.453; 0.544	0.569	0.516; 0.46; 0.54
		PAL	0.076	0.188 ; 0.149; 0.804	0.622	0.59 ; 0.569; 0.604	0.621	0.587 ; 0.565; 0.602
CIFAR100	MOBILENETV2	RMSP	0.083	0.22; 0.176; 0.98	0.676	0.588; 0.454; 0.659	0.672	0.588; 0.432; 0.65
		ADAM	0.049	0.305; 0.077; 2.502	0.684	0.579; 0.379; 0.653	0.687	0.578; 0.386; 0.651
		RADAM	0.049	0.314; 0.086; 2.599	0.684	0.578; 0.363; 0.659	0.681	0.572; 0.373; 0.649
		SGD	0.054	0.208 ; 0.068; 0.971	0.666	0.585; 0.517; 0.623	0.663	0.587; 0.514; 0.623
		PAL	0.059	0.231; 0.116; 2.928	0.702	0.653 ; 0.248; 0.678	0.697	0.638 ; 0.105; 0.675
CIFAR100	RESNET32	RMSP	0.266	0.425 ; 0.321; 0.758	0.637	0.608; 0.55; 0.621	0.638	0.609 ; 0.547; 0.621
		ADAM	0.254	0.766; 0.338; 2.754	0.637	0.558; 0.276; 0.619	0.636	0.561; 0.28; 0.61
		RADAM	0.272	0.807; 0.354; 1.426	0.639	0.563; 0.472; 0.622	0.639	0.56; 0.474; 0.616
		SGD	0.257	0.465; 0.317; 0.87	0.638	0.597; 0.555; 0.625	0.636	0.596; 0.551; 0.625
		PAL	0.387	0.51; 0.467; 2.53	0.635	0.609 ; 0.329; 0.623	0.632	0.594; 0.305; 0.613
TOLSTOI	RNN	RMSP	1.201	1.388 ; 1.32; 1.449	0.599	0.582 ; 0.561; 0.592	0.591	0.564 ; 0.553; 0.576
		ADAM	1.247	1.473; 1.379; 2.659	0.599	0.488; 0.327; 0.58	0.591	0.467; 0.262; 0.564
		RADAM	1.255	1.663; 1.424; 2.471	0.598	0.528; 0.313; 0.575	0.59	0.502; 0.31; 0.557
		SGD	1.248	1.562; 1.285; 2.277	0.599	0.539; 0.363; 0.594	0.591	0.532; 0.359; 0.585
		PAL	1.236	1.658; 1.317; 1.807	0.599	0.519; 0.496; 0.587	0.587	0.512; 0.47; 0.578
IMAGENET	DENSENET121	RMSP	5.694	6.9; 6.297; 6.9	0.153	0.001; 0.0; 0.077	0.148	0.0; 0.0; 0.074
		ADAM	1.965	6.901; 4.433; 6.924	0.529	0.001; 0.001; 0.265	0.527	0.001; 0.001; 0.264
		SGD	1.348	2.04 ; 1.694; 2.93	0.59	0.531 ; 0.447; 0.56	0.589	0.523 ; 0.435; 0.556
		PAL	2.111	2.799; 2.455; 4.644	0.501	0.405; 0.216; 0.453	0.499	0.405; 0.214; 0.452
IMAGENET	EFFICIENTNET	RMSP	6.174	13.731; 9.953; 17.007	0.406	0.207; 0.179; 0.306	0.055	0.019; 0.012; 0.037
		ADAM	0.801	5.554; 3.178; 5.969	0.677	0.569; 0.531; 0.623	0.67	0.335; 0.169; 0.502
		SGD	0.801	0.803 ; 0.802; 0.893	0.676	0.676 ; 0.667; 0.676	0.674	0.671 ; 0.664; 0.672
		PAL	0.94	1.138; 1.039; 1.215	0.674	0.66; 0.652; 0.667	0.672	0.657; 0.65; 0.665
IMAGENET	RESNET101	RMSP	5.833	10.087; 7.96; 10.715	0.452	0.428; 0.327; 0.44	0.384	0.078; 0.075; 0.231
		ADAM	1.713	3.194; 2.454; 5.081	0.638	0.618; 0.31; 0.628	0.586	0.3; 0.15; 0.443
		SGD	2.615	3.027; 2.821; 3.332	0.636	0.635 ; 0.635; 0.636	0.521	0.345; 0.299; 0.433
		PAL	0.572	0.99 ; 0.781; 1.109	0.642	0.601; 0.593; 0.622	0.639	0.592 ; 0.587; 0.615

C. Further experimental design details

C.1. Data Augmentation

We performed the following augmentations with a probability of 0.5 each on CIFAR10:

2 pixel padding and cropping, image rotation between 0° and 12° , left and right image flipping, change of hue, change of brightness, change of contrast, and cutout of a 16×16 square.

On CIFAR100 we used the same augmentations except of cutout of an 8×8 square instead of a 16×16 square.

On IMAGENET we again used the same augmentations except of an initial random crop to 224×224 pixels and cutout of a 56×56 square. For CIFAR10, CIFAR100 and IMAGENET all images were normalized by pixel-wise mean and variance.

For the War and Peace dataset we omitted augmentation.

C.2. Hyperparameter grid search

For our evaluation we used all combinations out of the following common used hyper-parameters:

ADAM and *RADAM*:

hyper-parameter	symbol	values
learning rate	λ	{0.1, 0.01, 0.001, 0.0001}
first momentum	β_1	{0.9}
second momentum	β_2	{0.999}
epsilon	ϵ	{ $1e-8$, 0.1, 1}

We did not vary the first or second momentum much since [18] states that the values chosen are already good defaults. The epsilon values are recommended by TensorFlow’s *ADAM* documentation [12].

SGD:

hyper-parameter	symbol	values
learning rate	λ	{0.1, 0.01, 0.001, 0.0001}
momentum	α	{0.8, 0.9, 0.99}

RMSPROP:

hyper-parameter	symbol	values
learning rate	λ	{0.1, 0.01, 0.001, 0.0001}
discounting	factor f	{0.9, 0.99}
epsilon	ϵ	{ $1e-8$ }

PAL:

hyper-parameter	symbol	values
measuring step size	μ	{1, 0.1, 0.01}
conjugate gradient factor	β	{0, 0.2, 0.4}
update step adaptation	α	{1, $\frac{1}{0.8}$, $\frac{1}{0.6}$ }
maximum step size	s_{max}	{1, 10}

In our experiments we worked with a factor $\frac{1}{\gamma} = \alpha$

D. Further line plots

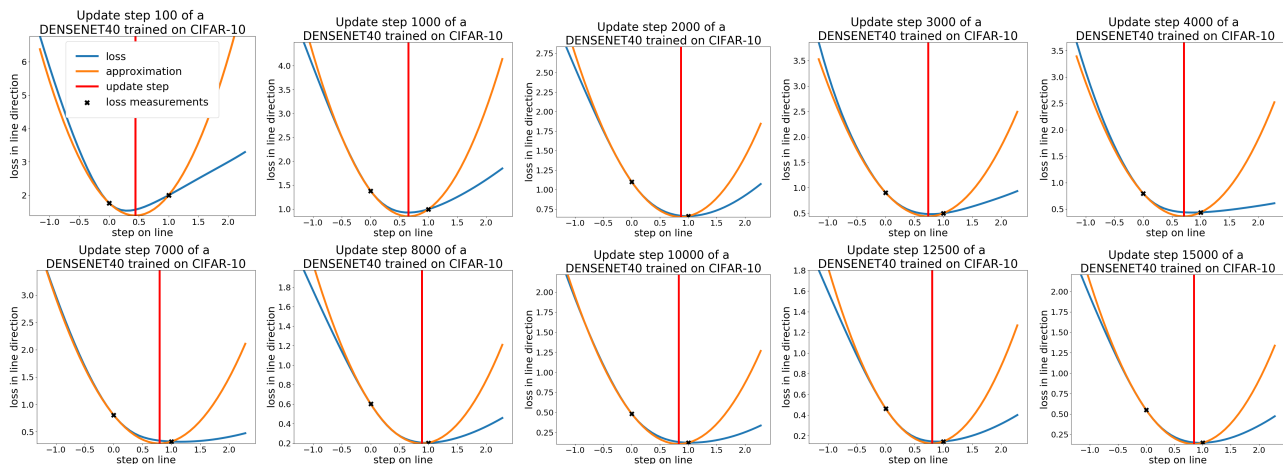


Figure 8: **DenseNet40** loss functions on lines in negative gradient direction (blue) combined with our parabolic approximation (orange) and the location of the minimum (red). The unit of the horizontal axis is the normalized gradient.

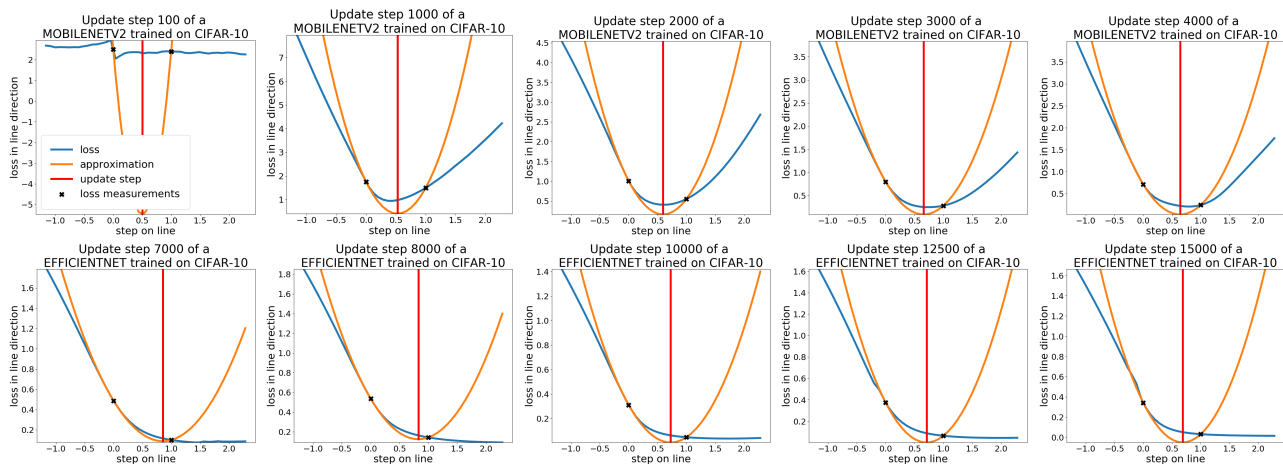


Figure 9: Loss line plots for **MobileNetV2**. For explanations see Figure 8.

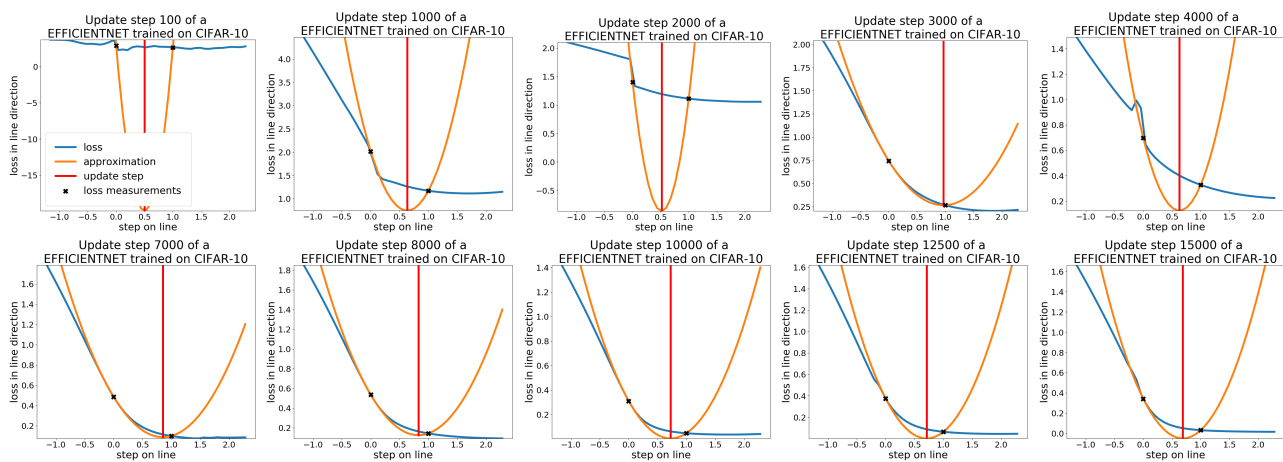


Figure 10: Loss line plots for **EfficientNet**. For explanations see Figure 8.